NOCTURNAL FLOW DYNAMICS AND PRESSURE-DRIVEN CHANNELING IN A DEEP VALLEY

Juerg Schmidli[1], Gregory S. Poulos[1], Fotini K. Chow[2], Megan H. Daniels[2]

[1] Earth Observing Laboratory, National Center for Atmospheric Research, Boulder, USA
[2] Department of Civil and Environmental Engineering, University of California, Berkeley, USA
E-mail: *schmidli@ucar.edu*

Abstract: This paper analyzes the nighttime flow dynamics and heat budget in a deep valley, California's Owens Valley, under weak to moderate synoptic forcing. Measurements from the Terrain-Induced Rotor Experiment (T-REX) reveal a pronounced valley-wind system with often non-classical flow structure. Here we focus on one particular event which was characterized by a mid-level layer of up-valley (southerly) flow between the low-level nocturnal down-valley flow and the synoptic north-westerly flow aloft. This layer of up-valley flow first occured at about 8 UTC, or midnight local time, at thereafter steadily increased in depth and strength. Our analysis is based on the T-REX measurement data and the output of high-resolution large-eddy simulations using the Advanced Regional Prediction System (ARPS). The ARPS output data are used to calculate the along-valley pressure gradient and the components of the heat budget of the valley atmosphere. The analysis shows that the mid-level up-valley flow is due to pressure-driven channeling overcoming the thermal forcing. Analysis of the heat budget shows that potential temperature advection is a dominant cooling factor during the evening transition and the onset of the main down-valley flow, but that turbulent heat flux divergence and radiation flux divergence are of comparable magnitude later on during the night.

Keywords: *ICAM, boundary layer, complex terrain, turbulence, thermally-driven flows, pressure-driven channeling*

1. INTRODUCTION

Valley and slope winds are an integral part of the mountain boundary layer. On the one hand, they may strongly modify the exchange fluxes between the land surface and the free atmosphere (Weigel et al., 2007). On the other hand, they may change the turbulence structure itself and, for example, suppress the growth of the mixed layer over the valley floor (Weigel et al., 2006). They also have a large influence on the nocturnal boundary layer over complex terrain (e.g. Monti et al., 2002). While the canonical properties of these flows are by now well established (Whiteman, 1990), their interactions with the larger-scale synoptic forcings are less well understood.

Observations of the Owens Valley wind system during the recent Terrain-induced Rotors Experiment (T-REX, held 1 March - 30 April 2006, near Independence in California) revealed frequent non-classical flow structure. One particular event, T-REX EOP 2, is the topic of this contribution. EOP 2 is characterized by the passage of a weak short-wave high-pressure ridge and the presence of some high cirrus clouds. Initially, a down-valley wind developed as expected. However, around midnight local time an eleveated layer of weak southerly up-valley flow appeared at $3000 - 3500$ m between the low-level down-valley flow and the upper-level north-westerly flow. This layer of up-valley flow steadily increased in strength and depth throughout the night until it eventually merged with the daytime up-valley flow. Our goal is to use large-eddy simulations of the flow in Owens Valley to investigate the mechanisms leading to this layered structure, and more generally to investigate the specific characteristics of the Owens Valley valley wind system.

2. SIMULATION SETUP

ARPS is applied in a one-way nesting mode, forced by the NAM analysis and nested down to 350 m horizontal resolution. The setup is similar to that of Chow et al. (2006) and Weigel et al. (2006). Key simulation parameters of each grid level are listed in Table 1. The topography for the coarser (finer) two grids was obtained from the USGS 30 (3) arc second topography dataset.

For surface characteristics we use the standard ARPS soil types and vegetation type classes. The 1 km soil type dataset is based on the state soil geographic (STATSGO) database, the 1 km vegetation type and NDVI datasets are based on the 1 km USGS North American datasets. From this input datasets ARPS derives the leaf

Table 1: Simulation parameters for the four grids.

(nx,ny,nz)	Δh	$\Delta z_{min}/\Delta z_{avg}$	$\Delta t/\Delta \tau$
(135,135,53)	9 km	50/500 m	10/10 s
(135,135,53)	3 km	50/500 m	2/2 s
(159,159,63)	1 km	40/400 m	1/1 s
(159,159,71)	350 m	30/350 m	1/0.2 s

area index (LAI), surface roughness (z_0), and the vegetation fraction used by the land-surface soil-vegetation model.

Initial and boundary conditions required to drive the 9 km run were derived from NAM analyses obtained through NOMADS. Simulations were carried out for 42 hours beginning at 12 UTC on 29 March. Output was stored at hourly intervals and used to force the subsequent nested grid simulations.

The coarse-resolution (14 km) surface data from NAM was found to be inadequate for our simulations (for instance, there was snow down in Owens Valley in the analysis, although the observed snowline was somewhere between 2500 and 3000 m). Therefore we initialized the simulations as follows: Soil temperature for all grids was set equal to the near-surface temperature, soil moisture was set to a constant soil saturation rate of 20%, and the snow cover was set to zero.

For the physical parameterizations standard ARPS options were used (Xue et al., 2001): a 1.5-order TKE turbulence closure model to represent turbulent mixing (Deardorff, 1980), stability and roughness-length dependent surface fluxes (Businger et al., 1971; Byun, 1990), a force-restore two-layer soil-vegetation model based on Noilhan and Planton (1989), and a sophisticated radiation package developed at NASA/Goddard Space Flight Center.

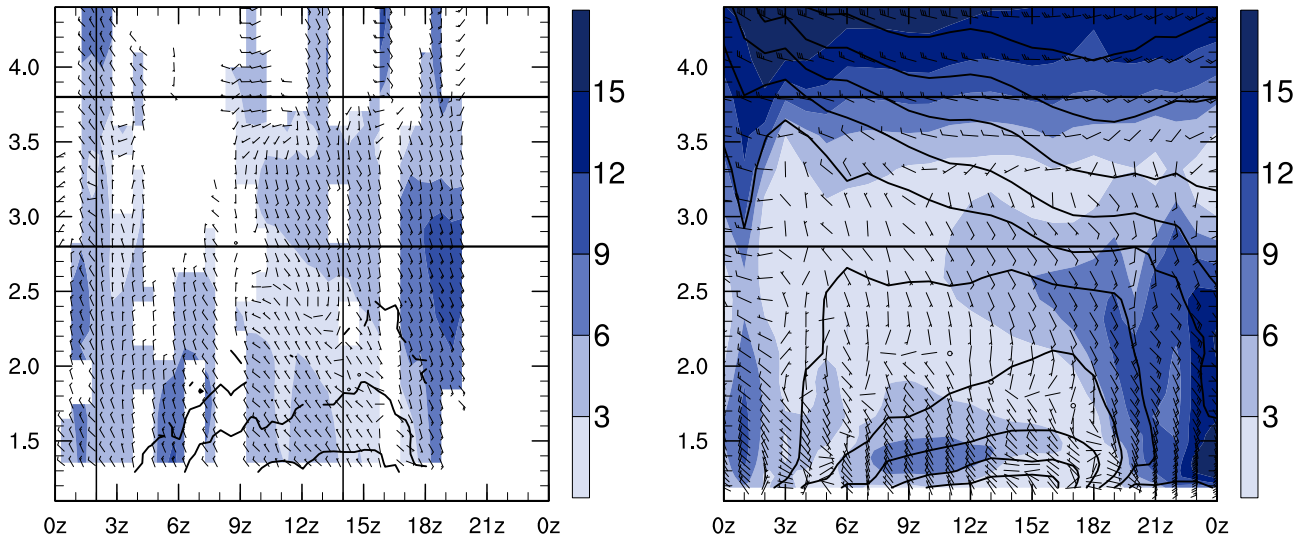

Figure 1: Time-height plot of wind direction (barbs), wind velocity (color) and potential temperature (contour lines) at the MISS Manzanar site for the wind profiler (a, left panel) and the model simulation (b, right panel).

3. FLOW STRUCTURE AND MODEL EVALUATION

From the wind profiler the following picture of the flow structure and evolution in Owens Valley can be deduced. During most of the day of the 29th the winds in the valley are weak (2-4 m/s, not shown). During the nighttime a persistent downvalley flow develops at the Manzanar site (as shown in Fig 1a). The speed of the flow is typically about 4 m/s, with a peak strength of 8-10 m/s around 6 UTC. The depth of the downvalley flow layer is reduced from more than 1 km during the early night hours to less than a few hundred meters by sunrise.

Starting as early as 9 UTC a layer of southerly up-valley flow develops at higher elevations within the valley atmosphere (around 3000 m MSL), and increases in depth and strength throughout the night. Above ridge level the wind increases in strength and turns to westerly.

Our simulations with ARPS are able to reproduce the main observed features. Figure 1 shows a comparison of the observed and simulated evolution of the valley flow at the Manzanar site during the night and the following day (until 4 pm PST). The three-layer structure with the downward propagation of the southerly flow layer is clearly reproduced. While the strength of the southerly flow is captured very well, the strength of the katabatic downvalley flow is somewhat overestimated by the model and its depth is slightly underestimated.

4. VALLEY-FLOW DYNAMICS

What is causing the layered structure? Our hypothesis is that the layering is the result of pressure-driven channeling interacting with local thermal forcing. Pressure-driven channeling refers to a valley wind forced by the component of the geostrophic pressure gradient along the valley's axis (Fiedler, 1983; Whiteman and Doran, 1993). In order to test this hypothesis a simulation with no radiation and no surface heat fluxes (NORAD) was carried out. Fig. 2 compares the result from NORAD with the reference simulation (REF). While the flow for NORAD and REF is very similar above about 2.5 km, there is no down-valley jet in the NORAD simulation. This experiment clearly demonstrates that the mid-level up-valley flow is due to large-scale forcing, while the low-level down-valley flow is the result of local thermal forcing.

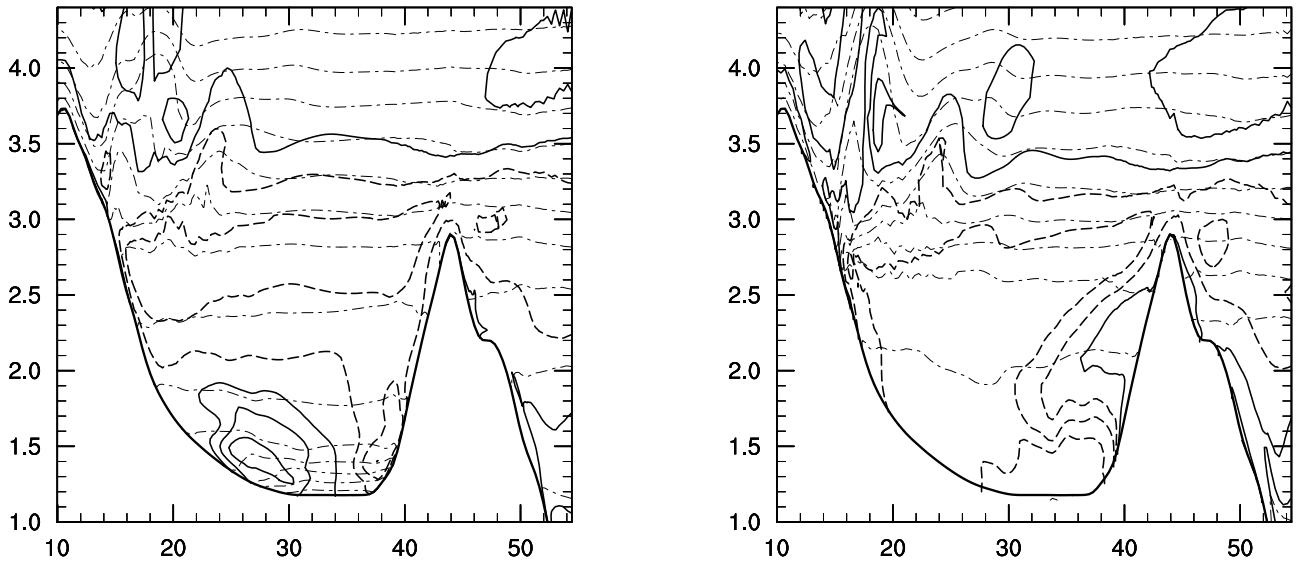

Figure 2: Along-valley wind component and potential temperature in a east-west valley cross section near Independence at 14 UTC (6 am local time) for REF (a, left panel) and NORAD (b, right panel).

The driving force for the along-valley wind is the horizontal along-valley pressure gradient. How is this pressure gradient related to the thermal forcing? Assuming that the flow is quasi-hydrostatic, the pressure gradient at an arbitrary level

$$\frac{1}{\rho_0}\frac{\partial p}{\partial x} = \frac{1}{\rho_0}\frac{\partial p_{\mathrm{ref}}}{\partial x} + \frac{gh}{\theta_0}\frac{\partial \overline{\theta}}{\partial x} \tag{1}$$

is given by the sum of the pressure gradient at some reference level and the horizontal gradient of the vertically integrated potential temperature deficit between the two levels (e.g. Mahrt, 1982). Fig. 3, which depicts the along-valley variation of pressure in the low- and mid-level flow layer, confirms that the valley flow is quasi-hydrostatic (good agreement between the solid and dashed curve). Furthermore it can be seen that the mid-level pressure gradient increases in strength between 8 and 14 UTC while the low-level pressure gradient decreases

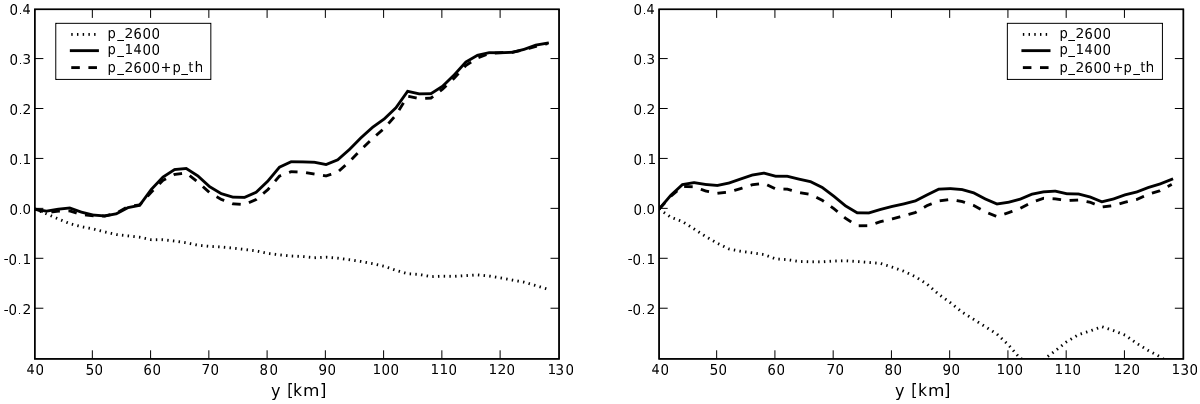

Figure 3: Along-valley variation of pressure at the center of the up-valley flow layer (2600 m) and at the center of the down-valley flow layer (1400 m) at 8 UTC (a, left panel) and 14 UTC (b, right panel). The abscissa denotes the north-south model coordinate from Owens Lake in the south ($y = 35$) to Bishop in the north ($y = 140$). The dashed line denotes the low-level pressure reconstructed from the mid-level pressure and the potential temperature deficit between the two levels.

in strength and is close to zero at 14 UTC. This explains the gradual increase in strength and depth of the mid-level up-valley flow layer.

Extending our analysis to the valley heat budget, we will further eloborate on the mechanisms leading to the specific characteristics of the Owens Valley wind system.

Acknowledgements: The support of the Swiss National Science Foundation (grant PA002-111427) for the first author is gratefully acknowledged. The National Center for Atmospheric Research funded by NSF for the computing time used in this research. The ground-based instruments teams from the university community and NCAR for their outstanding efforts at T-REX.

REFERENCES

Businger, J. A., J. C. Wyngaard, Y. Izumi, and E. F. Bradley, 1971: Flux-profile relationships in the atmospheric surface layer. *J. Atmos. Sci.*, **28**, 181–189.

Byun, D. W., 1990: On the analytical solutions of flux-profile relationships for the atmospheric surface layer. *J. Appl. Meteorol.*, **29**, 652–657.

Chow, F. K., A. P. Weigel, R. L. Street, M. W. Rotach, and M. Xue, 2006: High-resolution large-eddy simulations of flow in a steep Alpine valley. Part I: Methodology, verification, and sensitivity experiments. *J. Appl. Meteorol.*, **45**, 63–86.

Deardorff, J. W., 1980: Stratocumulus-capped mixed layers derived from a 3-dimensional model. *Boundary-Layer Met.*, **18**, 495–527.

Fiedler, F., 1983: Einige Charakteristika der Strömung im Oberrheingraben. Wiss. ber. meteorol. inst., Univ. Karlsruhe, 113–123 pp.

Mahrt, L., 1982: Momentum balance of gravity flows. *J. Atmos. Sci.*, **39**, 2701–2711.

Monti, P., H. J. S. Fernando, M. Princevac, W. C. Chan, T. A. Kowalewski, and E. R. Pardyjak, 2002: Observations of flow and turbulence in the nocturnal boundary layer over a slope. *J. Atmos. Sci.*, **59**, 2513–2534.

Noilhan, J., and S. Planton, 1989: A simple parameterization of land surface processes for meteorological models. *Mon. Wea. Rev.*, **117**, 536–549.

Weigel, A. P., F. K. Chow, and M. W. Rotach, 2007: The effect of mountainous topography on moisture exchange between the "surface" and the free atmosphere. *Boundary-Layer Met.*, in press.

Weigel, A. P., F. K. Chow, M. W. Rotach, R. L. Steet, and M. Xue, 2006: High-resolution large-eddy simulations of flow in a steep Alpine valley. Part II: Flow structure and heat budgets. *J. Appl. Meteorol. and Climatol.*, **45**, 87–107.

Whiteman, C. D., 1990: Observations of thermally developed wind systems in mountainous terrain. *Atmospheric Processes over Complex Terrain*, *Meteorological Monographs*, No. 23, Amer. Meteor. Soc., 5–42.

Whiteman, C. D., and J. C. Doran, 1993: The relationship between overlying synoptic-scale flows and winds within a valley. *J. Appl. Meteorol.*, **32**, 1669–1682.

Xue, M., K. K. Droegemeier, V. Wong, A. Shapiro, K. Brewster, F. Carr, D. Weber, Y. Liu, and D. Wang, 2001: The Advanced Regional Prediction System (ARPS) — A multi-scale nonhydrostatic atmospheric simulation and prediction model. Part II: Model physics and applications. *Meteorol. Atmos. Phys.*, **76**, 143–165.